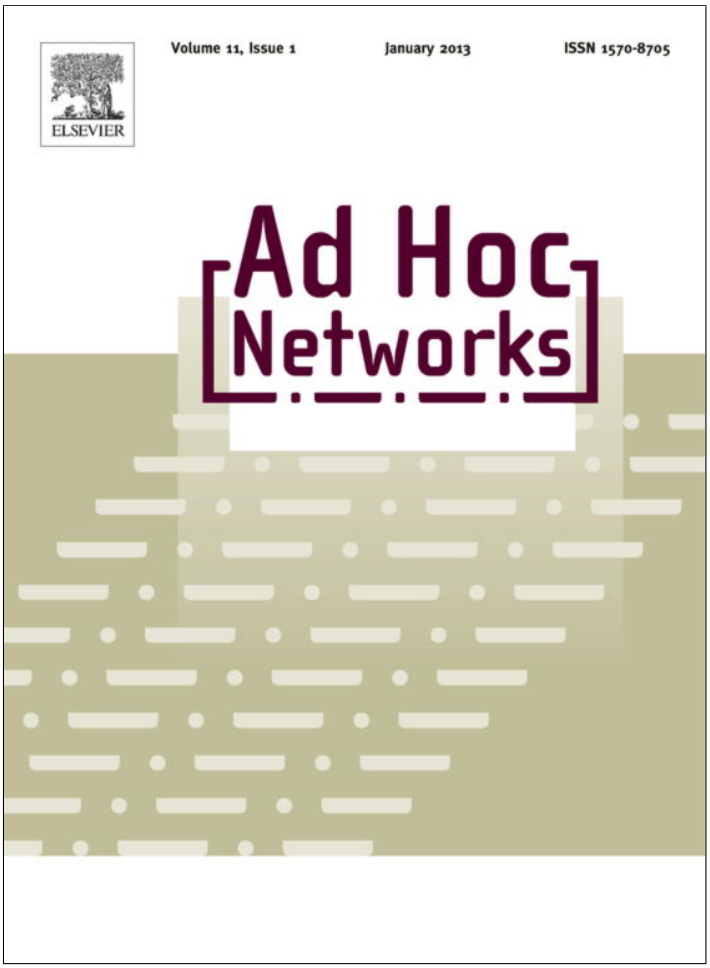

Ad Hoc Networks 11 (2013) 442–452

Contents lists available at SciVerse ScienceDirect

Ad Hoc Networks

journal homepage: www.elsevier.com/locate/adhoc

Accurate time synchronization of ultrasonic TOF measurements in IEEE 802.15.4 based wireless sensor networks

C. Medina, J.C. Segura *, A. de la Torre

Centro de Investigación en Tecnologías de la Información y las Comunicaciones, Universidad de Granada (CITIC-UGR), C/ Periodista Rafael Gómez, n° 2 de Granada, 18071 Granada, Spain
Dpto. Teoría de la Señal, Telemática y Comunicaciones (TSTC), ETSI de Ingenierías Informática y de Telecomunicación, Univeridad de Granada, C/ Periodista Daniel Saucedo Aranda S/N, 18071 Granada, Spain

ARTICLE INFO

Article history:
Received 18 February 2012
Received in revised form 19 June 2012
Accepted 23 July 2012
Available online 8 August 2012

Keywords:
Network time synchronization
Ultrasonic pseudorange measurement
Wireless sensor networks
Local positioning systems (LPSs)
Time Division Multiple Access (TDMA)

ABSTRACT

This paper discusses the problem of accurate time synchronization of wireless sensor networks (WSNs) used in applications in which a physical phenomenon must be monitored through periodical sampling. In some applications incorrect time synchronization can significantly degrade the system precision. This is for example the case of local positioning systems (LPSs) using ultrasonic time of flight (TOF) measurements for pseudorange estimation. The nodes clock drifts and the random variations of the start time used in each measurement are the two main error sources. In this work a Time Division Multiple Access (TDMA) synchronization algorithm is presented to overcome these problems for WSN using the IEEE 802.15.4 standard. The algorithm is able to compensate for the mentioned error sources in an easy and effective way. Experimental results for an implementation of an ultrasonic pseudorange measurement system between wireless nodes show the effectiveness of the proposed algorithm.

1. Introduction

Time synchronization between networked devices is essential in many applications, particularly in wireless sensor networks (WSNs) designed to measure a physical phenomenon based on periodic sampling. In most cases sample times are used to process the measurements and therefore the obtained precision is conditioned by the time synchronization of the network. This is for example the case of pseudorange measurements in ultrasonic positioning systems. A precise knowledge of the ultrasonic pulses emission times is needed to accurately estimate the time of flight (TOF) and the corresponding pseudorange. If emitter and receiver clocks are not accurately synchronized, the precision of the estimated pseudoranges is significantly degraded.

The motivation of this work arises from the need to solve the synchronization problems in TELIAMADE [1,2], a local positioning system (LPS) recently developed by our research group. This system consists of wireless ultrasonic sensors interconnected using the ZigBee protocol [3]. Distance measurements are estimated from the TOF of an ultrasonic signal between two network nodes, and ZigBee protocol is used to over-the-air configure and control the WSN.

The ZigBee standard is a communication protocol designed for systems with low power requirements, low data rate and secure communication that is appropriate for WSN. Unlike other standards, it has a lower complexity protocol stack that results in a lower memory and computational resources demand. ZigBee implements IEEE 802.15.4 standard [4] in its medium access control (MAC)

* Correspondig author at: Dpto. Teoría de la Señal, Telemática y Comunicaciones (TSTC), ETSI de Ingenierías Informática y de Telecomunicación, Univeridad de Granada, C/ Periodista Daniel Saucedo Aranda S/N, 18071 Granada, Spain. Tel.: +34 958 243283; fax: +34 958 240831.
E-mail addresses: cmedina@ugr.es (C. Medina), segura@ugr.es (J.C. Segura), atv@ugr.es (A. de la Torre).

1570-8705/$ - see front matter © 2012 Elsevier B.V. All rights reserved.
http://dx.doi.org/10.1016/j.adhoc.2012.07.005

and physical layer (PHY), typically operating at 2.4 GHz with a maximum data transfer rate of 250 Kbps.

Ultrasound location systems based on TOF provide accurate estimation of distances (and positions using multilateration algorithms) compared with other technologies. Systems based on radio signals require less infrastructure than other technologies but offer lower precision: from tens of centimeters in UWB systems using Time of Arrival (TOA) measurements [5], to several meters for systems using RSSI measurements WiFi [6], ZigBee [7], and RFID [8]. Advances in machine vision make achieving accuracies of several centimeters possible [9] at the cost of using an expensive infrastructure, low modularity and high processing requirements. Ultrasound technology also offers some advantages for locations purposes such as a slow signal propagation speed, no penetration of walls, lack of regulatory control or low cost transducers. It allows obtaining centimeter or even sub-centimeter accuracies with a relatively low processing resources demand. The time for the ultrasonic signal to travel the distance between a sending node and a receiving node is used for the estimation of the distance between these two nodes considering the sound propagation speed. This requires a proper synchronization of the network, so that the transmission and reception nodes share a common time reference.

TELIAMADE is aimed at solving the limitations of a previous location system called ATLINTIDA [10]. This system is based on a set of ultrasonic transmitters and receivers nodes controlled from a personal computer (PC) where the estimation process of the mobile node position is performed. The wired connection between the transmitters nodes and the PC makes difficult and costly the deployment of the system. The ultrasonic signal at the receiver is wirelessly transmitted to the PC using an analog FM radio link. Therefore, a different FM channel is needed for each receiver, which results in a scalability problem for the system. This centralized design of the system can lead to the overload of the PC for a not very high number of receivers nodes. Finally, the use of Amplitude-shift keying (ASK) modulation for transmission of the ultrasonic signal makes the system not too much robust to noise and does not allow the simultaneous signal transmission from multiple transmitters. In TELIAMADE system both generation and reception of the ultrasound signal are performed on the nodes so that the workload of the master node is reduced. The hardware design of nodes allows working with digital signals and offers the possibility of implementing more efficient and robust modulation techniques. The wireless connection between nodes is based on a shared digital radio link. This makes easier the deployment of the system and reduces costs. However the wireless connection causes serious synchronization problems that can reduce the system accuracy. This paper discusses these problems and proposes an efficient method to compensate their effects.

In systems with a wired connection between devices, synchronization can be easily achieved through electrical pulses, such as in the ATLINTIDA [10] system. In contrast, in a wireless architecture it is common to use pulses of radio frequency (RF) to provide such synchronization. In the literature we find several examples of ultrasonic LPSs based on the measurement of TOF ultrasonic signal which use RF to provide synchronization, taking advantage of negligible propagation delay of this signal. Some of these systems are Active Bat [11], Cricket [12] or Dolphin [13] (for which accuracies of a few centimeters are reported) and more recently 3D-Locus [14,15] (with sub-centimeter reported accuracy). This requires the existence of specific RF modules in the nodes of the network (in addition to that used for data transmission and control) to provide synchronization.

For TELIAMADE system we propose to use the same radio interface (e.g. 802.15.4) for both data transfer and synchronization purposes. The proposed synchronization scheme is able to maintain a common time reference for all network nodes. Using this common time base, accurate TOF measurements can be obtained without the need of a specific radio link for time synchronization. The proposed algorithm allows the system to perform regularly scheduled measurements without the intervention of a supervisor node, maintaining sub-centimeter accuracy. It is based on a Time Division Multiple Access (TDMA) approach to share the ultrasonic channel. Using this approach, the network nodes can be programmed to start transmission or reception of ultrasonic pulses at given time instants. Using this approach, network time synchronization can be maintained within ±1 μs even under condition of relative clock drifts between network nodes as large as 50 parts-per-million (ppm). The synchronization algorithm is based on an estimation of the relative clock drift of each node. This estimation is obtained from time stamps of synchronization messages sent by the network coordinator at a rate of less than 10 packets per minute.

The rest of the paper is organized as follows. In Section 2 a general overview of the TOF measurement system is presented. Section 3 describes the proposed TDMA synchronization scheme. The main sources of variation causing de-synchronization of the nodes are studied; in particular random variations due to different processing times in transmitter and receiver nodes and local time variations due to drifts of the clock of the nodes are considered. In Section 4 a solution is proposed to compensate for the different processing time in the nodes, and in Section 5 the compensation for the local clock drifts is presented. In Section 6 the proposed algorithm is evaluated. Results are presented to evaluate the impact of the different error sources in the system accuracy and confirm the proper operation of the proposed algorithm. Main features of the proposed system are discussed. Finally, in Section 7 the main conclusions of this work are summarized.

2. TOF measurement system description

In this work we consider that the WSN nodes are part of a ZigBee network with a star topology. ZigBee messages are used for both data transfer between nodes and also for synchronization purposes. Configuration and control of all network nodes is based on a simple message passing system.

Each of the nodes is equipped with a microcontroller (PIC18F4620) [16], a radio chip (CC2420) [17] implementing

the 802.15.4 physical layer and a couple of ultrasonic transducers (transmitter and receiver). Therefore, a given node can be configured to transmit or receive an ultrasonic signal at a given time. TOF estimations are obtained by measuring the time delay between the transmission and reception of a 1 ms ultrasonic pulse.

In TELIAMADE, ultrasonic transducers (400ST/R120) [18] with a center frequency of 40 kHz and a 6 dB bandwidth of 2 kHz are used. Generation of an ultrasonic burst is done using the EUSART of the microcontroller. A sequence of alternating 0 and 1 bits is generated at a baud rate of twice the nominal frequency of the transducer (i.e. 80 Kbps) with an appropriate length (e.g. a 1 ms burst requires the transmission of a sequence of 80 alternating bits). The EUSART output drives the transducer generating the desired ultrasonic burst.

The signal is buffered in a digital hex inverter (MC14049UB) [19] using a push–pull configuration in order to increase the transmitted signal amplitude. In reception, the signal is amplified and band-pass filtered before being sampled and digitized using the *A*/*D* converter of the microcontroller. This signal conditioning stage is implemented using a dual operational amplifier (LMC6482IN) [20] and some passive components (resistors and capacitors). The overall complexity and cost of the additional hardware is very low in comparison with the ZigBee hardware. Fig. 1 shows the hardware design of the nodes. Computation of the TOF is performed using a digital correlator to obtain a precise estimation. The receiver samples the ultrasonic signal and stores the samples in a memory buffer. To allow the reception of a 1 ms burst traveling a distance of 10 m it is necessary to sample the ultrasonic channel for at least 30 ms. A 10 bits analog-to-digital converter is used in our current implementation. A quadrature band-pass sampling scheme [21,22] is used to reduce the required memory and processing resources. For a 40 kHz carrier, the receptor can be operated at sampling frequencies of 32 kHz, 17.78 kHz or 12.31 kHz (single side reception bandwidths of 8 kHz, 4.45 kHz and 3.08 kHz). The corresponding buffer sizes are 1920, 1067 and 738 bytes respectively (assuming two byte samples). Parabolic interpolation [23] of the correlator output around the position of the maximum is used to obtain a time resolution significantly better than 1/2 sample.

In order to obtain an accurate estimation of the TOF the receiver needs to know the time instant when the transmitter starts the generation of the ultrasonic pulse. A possible solution is to use a ZigBee message to fire the TOF measure simultaneously in both the transmitter and the receiver. In this way, the receiver can estimate the TOF as the time delay between the start of the reception and the time the ultrasonic pulse is detected. For a single TOF measurement between a pair of nodes (transmitter and receiver) a simple implementation is as follows: (1) the network coordinator sends a broadcast message that is simultaneously received by both the transmitter and

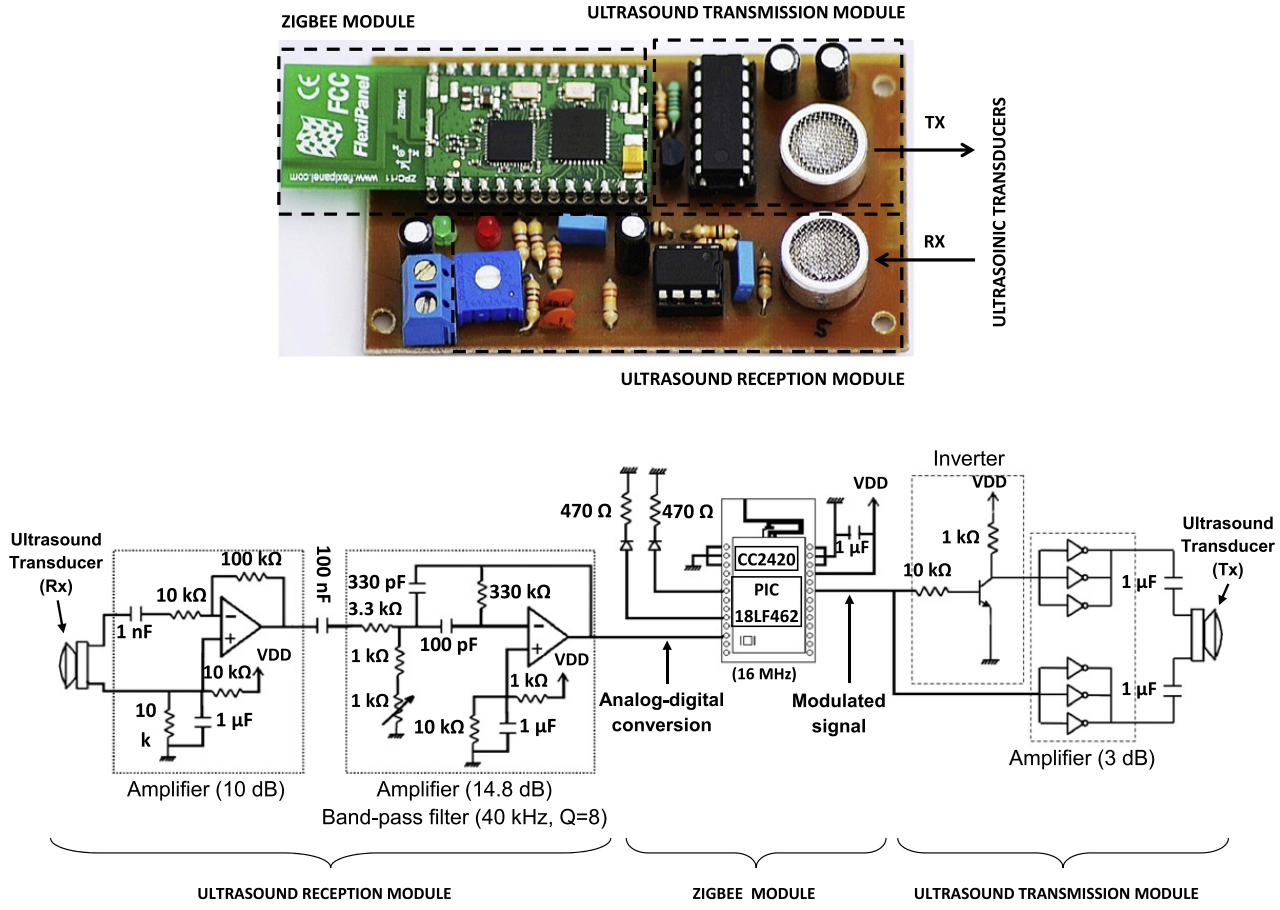

Fig. 1. Picture (top) and hardware design (bottom) of a TELIAMADE node.

receiver nodes; (2) the reception of this message fires the generation of the ultrasonic pulse in the transmitter node and the start of the reception process in the receiver node; (3) the receiver node samples the ultrasonic pulse and stores the samples in memory. The digital correlator is then used to find the start time of the sampled pulse. The TOF is estimated as the difference between this time and the start of the sampling process.

Although this scheme guarantees adequate time synchronization and therefore correct TOF estimates, it has some disadvantages. First, it requires that all network nodes remain actively listening the radio interface. This forces nodes not to be in sleep mode with the consequent increase in power consumption. Second, this scheme involves high network traffic, especially considering situations with high measurements rate.

In order to avoid the above mentioned problems, next subsection presents an alternative synchronization mechanism designed to operate at a much lower packet transmission rate. The solution introduces some timing issues that will described later in Section 3.1.

3. Low rate synchronization

A more efficient solution is to use a periodic pre-scheduled measurement scheme based on a Time Division Multiple Access (TDMA) approach to share the ultrasonic channel. Using this approach, the network nodes can be programmed to start transmission or reception of ultrasonic pulses at given time instants that are specified using a temporal structure like the one shown in Fig. 2. In this example, the TDMA structure is organized in periods of 6.4 s which we will refer to as a multiframe. The beginning of each multiframe is signaled by the network coordinator by sending a synchronization message (Msync) which all network nodes receive at virtually the same time. This provides a common time base for all network nodes, from which it is easy to schedule the precise time instant at which a given node must begin the transmission or reception of an ultrasonic pulse. Each multiframe is divided into 32 frames of 200 ms. Typically, one TOF measurement is performed at the beginning of every single frame of the multiframe. This allows performing up to 5 measurements per second. This frame duration allows enough time for the receiver node to sample, store and process ultrasonic bursts of 1 ms traveling a distance of several tens of meters.

In a periodic measurement scenario, each transmitter node is assigned one or more frames in which the node is active. The receiver is scheduled to sample the ultrasonic channel every new frame. In this way, a maximum of 32 different pseudoranges can be measured every 6.4 s. Changing the number of frames and the frame duration, the TDMA structure can be configured to fit other measurement scenarios. Note that using the above described scheme, the synchronization messages rate is reduced in a factor of 32 (synchronization messages are sent by the coordinator every 32 frames; instead of sending one message for every new measurement). This scheme also allows the nodes to put its radio transceiver in an idle state most of the time (with the consequent power saving) and only activate it to receive the synchronization message at the beginning of each multiframe.

In order to find the beginning of a given frame in the multiframe, each network node maintains a local tick counter that is reset at the beginning of each multiframe. At any given time instant, each node can compute the frame number and the time offset within the frame as follows. Consider Δt as the time offset from the reception of the synchronization message at the beginning of the multiframe. Then, the frame number is computed as

$$n_F = \left\lfloor \frac{\Delta t}{T_F} \right\rfloor \quad (1)$$

where T_F stands for the frame duration. The time offset from the beginning of the current frame is

$$\Delta t_o = \Delta t - n_F T_F \quad (2)$$

In a general scenario, each transmitter node starts the ultrasonic pulse generation at the beginning of a given frame of the multiframe. The receptor node starts the reception process of the ultrasonic pulse at the beginning of the same frame, which guarantees that both processes start at the same time (i.e. synchronously). The time elapsed since the beginning of the reception process until the pulse is detected by the correlator is therefore the TOF of the ultrasonic signal.

3.1. Timing issues

The synchronization error is lower bounded by the time resolution of the nodes clock T_o as follows. When a transmitter node is synchronized with the coordinator, the error between their respective clocks can be assumed to be

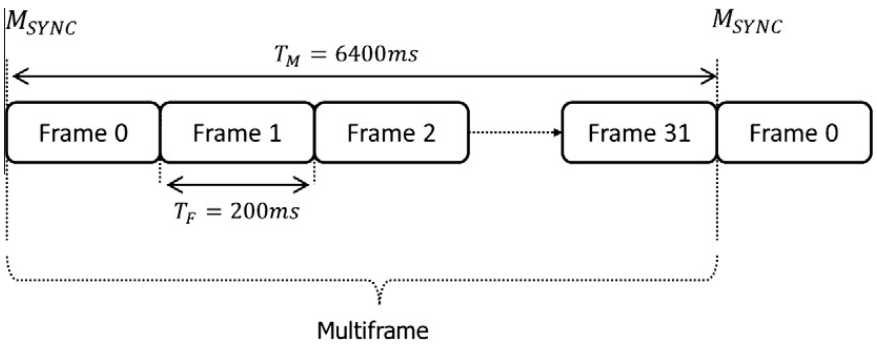

Fig. 2. TDMA temporal structure used for measurement scheduling.

uniform in the range $\pm T_o/2$ and its standard deviation will be $T_o/\sqrt{12}$. The same holds for the error between the receiver node clock and the coordinator clock. The synchronization error between the transmitter and receiver is the difference of two independent uniform distributed random variables and will have a standard deviation

$$\sigma_{CLK} = \frac{\sqrt{2}T_o}{\sqrt{12}} = \frac{T_o}{\sqrt{6}} \tag{3}$$

For a typical value of $T_o = 1$ μs, the standard deviation of the timing error will be $\sigma_{CLK} = 0,41$ μs. Assuming this as the unique source of error in the pseudorange estimations, and for a typical sound speed of $c = 340$ m/s, the precision of pseudorange measurements will be limited to 0,14 mm. This is sufficient for most applications, including those requiring sub-centimeter accuracies. In practice, there are other effects that cause greater synchronization errors leading to greater pseudorange errors. Two important of such effects are described now.

Both ultrasonic transmission and reception processes are digitally implemented by the node microcontroller. Depending on the node configuration (as transmitter or receiver) the number of executed instruction cycles before the start of transmission and reception of the ultrasonic signal are different. The time elapsed from the start of the transmission (reception) process until the actual beginning of transmission (reception) may vary depending on the configuration and node computational load. These delays cause random time variations that lead to random errors of TOF estimations. A solution to this problem is described in Section 4.

Most microcontrollers have clocks driven by crystal oscillators, and relative frequency variations in the order of 10–100 ppm around its nominal value is common for commercial crystals. This relative clock drift can yield to significant variations when measuring long time intervals. This is the situation of managing the TDMA structure used for synchronization, in which intervals on the order of several seconds need to be measured. The time error due to a 50 ppm drift during the measurement of a 6.4 s interval (the multiframe duration) is 320 μs. Such a timing error will lead to a pseudorange error of 10.9 cm at 340 m/s. In Section 5 we will present a solution to this problem.

4. Compensation for the difference between transmission and reception start times

Both generation (in transmission) and sampling (in reception) of ultrasonic signals are performed using interrupt driven routines of the nodes microcontrollers. To precisely synchronize these processes, it is necessary to activate the periodic interrupts at the same time in both transmitter and receiver nodes. Before enabling the interrupt driven process, the node must perform several operations to set up the microcontroller peripherals involved in the operation (the EUSART is used for ultrasonic signal generation for transmission and the analog-to-digital converter for the reception). This involves the execution of a different number of instruction cycles and therefore a different time interval that also depends on the microcontroller load. A random time delay occurs between the activation of the transmission or reception routines and the actual time at which the corresponding process begins (i.e. first interrupt is fired).

In Fig. 3, a schematic timing diagram of the transmission and reception processes is shown. Even when the two processes are fired at a common time t_{ref}, there exists a delay Δp between the actual beginning of the transmission and reception process (i.e. the time the first signal sample is generated $t_{int}\{Tx\}$ in the transmitter node and the time the first signal sample is acquired $t_{int}\{Rx\}$ in the receptor node). Δp is a random time interval that depends on the current node configuration and load.

To overcome the lack of synchronization caused by the previously described situation, we use a fixed common delay τ from the reference time t_{ref} (i.e. the beginning of the scheduled frame for the node) before enabling the microcontroller interrupt services. For transmission, once reached t_{ref} the node sets up the adequate peripherals (ending at time $t_{int}\{Tx\}$). But instead of enabling the interrupt driven process, it waits until t'_{ref} to do this. A similar procedure is followed for reception (now involving times $t_{ref}, t_{int}\{Rx\}$ and t'_{ref}). Hardware timers are used to implement the required delays ($t'_{ref} - t_{int}\{Tx\}$ for transmission and $t'_{ref} - t_{int}\{Rx\}$ for reception).

The time interval τ is selected to allow both transmission and reception nodes to finish its configuration. This interval is selected based on the experimental measurements of $t_{int}\{Tx\} - t_{ref}$ and $t_{int}\{Rx\} - t_{ref}$. A value greater than the maximum of these delays must be selected to ensure a proper operation of the algorithm. Section 6 discusses the experimental selection of an appropriate value for τ. Transmission and reception processes are therefore started synchronously at time instant

$$t'_{ref} = t_{ref} + \tau \tag{4}$$

where t_{ref} is computed based on the assigned frame n_F and the time of the multiframe start t_n

$$t_{ref} = t_n + n_F T_F \tag{5}$$

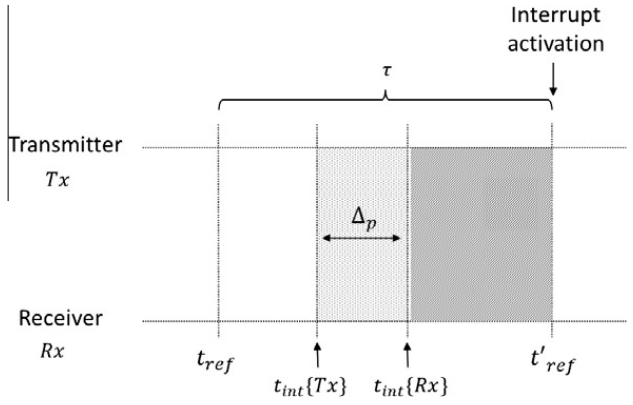

Fig. 3. Illustration of the transmission/reception timing. t_{ref} is the time when a given node is scheduled to begin its processing routine (transmission or reception). $t_{int}\{Tx\}$ and $t_{int}\{Rx\}$ refer to the time instants when the processing interrupt is activated in the transmitter and receiver nodes respectively when no compensation is used. τ is a fixed delay and t'_{ref} is the time when both transmission and reception interrupt driven routines are synchronously started when compensation is used.

5. Clock drift compensation

The synchronization error caused by the clock drifts linearly increases with the relative drift and the time interval that is measured. For example, a 10 ppm clock drift in a 3 s interval introduces an error of 30 μs (or 10.2 mm at 340 m/s). We propose to compensate for the clock drifts by using a common time base for all network nodes instead of using its own local clock. In our implementation, the network coordinator time is used as reference. This approach is a variant of the algorithm proposed in [24]. Each node performs an estimation of the common reference time (the coordinator time) using a linear transformation of its local time. In this way, all nodes share a common time base avoiding the effects of each node clock drift. For sake of simplicity we present here the algorithm as if only one node clock is going to be synchronized with the network coordinator clock.

A first order linear model is used to relate the coordinator time t_c and the node time t_n

$$t_c = t_o + (1+\alpha_n)t_n \tag{6}$$

where α_n is the relative clock drift and t_o a fixed offset between the node and the coordinator clocks.

Every time interval measured with a node n clock is related to the equivalent time interval measured with another node m clock in a similar way.

$$\Delta t_c = (1+\alpha_n)\Delta t_n \tag{7}$$
$$\Delta t_c = (1+\alpha_m)\Delta t_m \tag{8}$$
$$\Delta t_n = (1+\alpha_{mn})\Delta t_m \tag{9}$$

where

$$\alpha_{mn} = \frac{\alpha_m - \alpha_n}{1+\alpha_n} \tag{10}$$

α_n and α_m are the clock drift of nodes n and m relative to the coordinator clock and α_{mn} is the clock drift of node m relative to the node n clock.

5.1. Clock drift estimation

To compute the drift of node n relative to the coordinator clock, at least to couples of time stamps (t_c, t_n) are required. This information is obtained from the synchronization messages the coordinator sends at the beginning of every multiframe. Consider $(t_c(k), t_n(k))$ as the time stamps obtained from the coordinator and node clocks at the beginning of the multiframe number k, and $(t_c(k-1), t_n(k-1))$ the corresponding time stamps for the previous multiframe. An estimation of the relative clock drift of the node at the current multiframe can be obtained as

$$\hat{\alpha}_n = \frac{t_c(k) - t_c(k-1)}{t_n(k) - t_n(k-1)} - 1 \tag{11}$$

Obtaining the time stamp $t_n(k)$ is easy. It only requires retrieving the local clock time at the reception of the synchronization message. Obtaining the corresponding coordinator time is more difficult because it is the time when the coordinator has sent the synchronization message. In our current implementation of the protocol two consecutive synchronization messages are send by the coordinator at the beginning of each multiframe as illustrated in Fig. 4. From the first message, only the reception time stamp $t_n = T_H$ is used (which is measured with the node clock). In the second message payload, the coordinator sends the time stamp $t_c = T_C$ corresponding to the time instant the previous message was sent (measured using the coordinator clock). Therefore, t_n and t_c are time stamps corresponding to a common time instant (propagation time of the RF signal is neglected) but measured using the node and coordinator clocks respectively. In this way, each network node can retrieve the needed time stamps used by the drift estimation Eq. (11).

To implement this algorithm a minor modification of the MAC layer is needed to record the times just at the beginning of the reception of a radio packet and just at the end of the transmission of a radio packet. In TELIAMA-

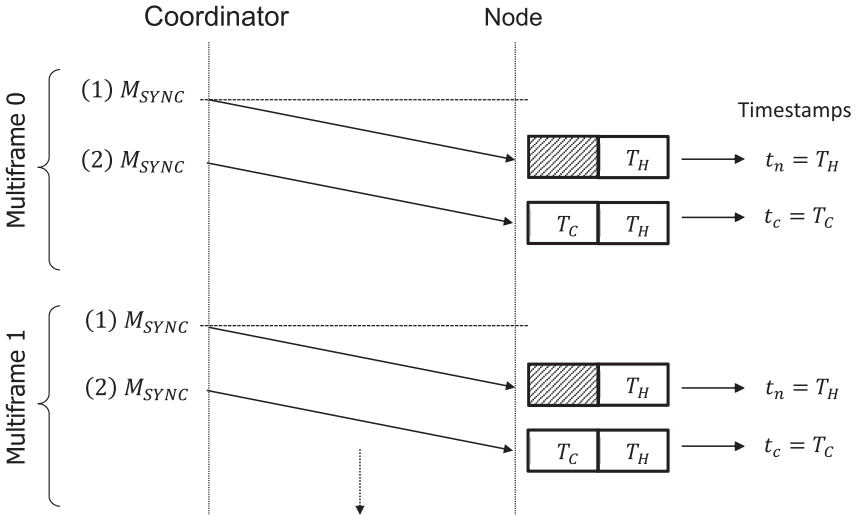

Fig. 4. Sequence of synchronization messages. T_H field is the time stamp of message reception filled by the node MAC layer. T_C field is the payload of the message only used in the second synchronization message.

DE system, the MAC layer code of the ZigBee stack is modified to record these time stamps.

Once the relative clock drift is estimated, every time interval measured with the node local clock can be easily converted to the coordinator clock. If Δt_n is a time interval measured using a given node clock, the corresponding time interval measured with the coordinator clock can be obtained using the estimated drift at the current multiframe as

$$\Delta \hat{t}_c = \Delta t_n (1 + \hat{\alpha}_n) \tag{12}$$

Using this relation, all time intervals measured with the local clock of the nodes are converted to the coordinator clock providing a common time base for all network nodes.

5.2. Implementation details

To show how clock drift compensation is implemented, let us consider the situation of a TOF measurement between a pair of nodes that is scheduled to be performed at the beginning of frame n_F of the multiframe. When no drift compensation is used, each node n (either emitter E or receiver R) performs the nominal delay $n_F T_F$ using its own clock. If we express this value in a common time base (e.g. the coordinator time base) it will be different for each node due to its relative clock drift

$$(\Delta t_n)_c = n_F T_F (1 + \alpha_n) \tag{13}$$

and therefore the synchronization error between the beginning of the transmission and reception processes will be

$$(\Delta t_E)_c - (\Delta t_R)_c = n_F T_F (\alpha_E - \alpha_R) \tag{14}$$

causing an incorrect TOF estimation.

To avoid this problem each node n pre-scales the nominal delay $n_F T_F$ using its α_n value as $\widehat{n_F T_F} = n_F T_F/(1 + \alpha_n)$. When each node implements this new delay using its local clock, the resulting value expressed in the coordinator time base will be

$$(\widehat{\Delta t_n})_c = \widehat{n_F T_F}(1 + \alpha_n) = \frac{n_F T_F}{(1 + \alpha_n)}(1 + \alpha_n) = n_F T_F \tag{15}$$

which is independent of the clock drift and therefore equal for all nodes; effectively avoiding the synchronization error.

6. Results and discussion

The above described synchronization algorithm has been tested in TELIAMADE local positioning system. The configuration used consists of a coordinator node and five end nodes. The coordinator is connected to a PC via an RS232 interface and provides a gateway between the user application running in the PC and the network nodes. Through this gateway the network administrator can configure the operation of end nodes by sending ZigBee messages (commands). The coordinator clock is taken as reference for measuring the clock drift of other network nodes. The compensation of the clock drifts is done by converting the time measurements made with the local clocks of the nodes to the time base of the coordinator. This provides a common time base and therefore compensates clock drift effects in TOF measurements.

In this section, experimental results showing the effectiveness of the proposed synchronization scheme are shown. In Section 6.1 we present the results of applying the compensation for the delay in the start of the measurement interrupt. In Section 6.2 we show the results of applying the compensation of clock drifts. Finally, in Section 6.3 the main features of the proposed TOF measurement system are summarized.

6.1. Compensation for the difference between transmission and reception start times

In Section 4 a description of the synchronization problem related to random delays at the beginning of transmission and reception of ultrasonic signals was presented, along with the proposed solution. In this section we provide experimental quantification of these effects and show how the proposed solution is able to effectively remove it.

To this purpose, we first performed a set of measurements involving all five end nodes. Each node was alternatively configured as transmitter and receiver; and for each configuration 200 measurements were obtained of time stamps t_{ref}, t_{int} and t'_{ref} as defined in Section 4 and Fig. 3. t_{int} corresponds to either $t_{int}\{Tx\}$ or $t_{int}\{Rx\}$ depending on the configuration as transmitter or receiver of the considered node. The time stamps are obtained from the local node clock with a resolution of 1 μs. A total number of 1000 measurements are obtained for each configuration (*Tx* and *Rx*). Table 1 shows the mean values, standard deviation, minimum and maximum values of delays with and without using the compensation scheme previously described. First row shows the mean delay values for nodes configured as transmitter (*Tx*) or receiver (*Rx*); second row shows the standard deviation and third and fourth rows show the minimum (*min*) and maximum (*max*).

To compensate for this delay, τ value is selected taking into account the experimental measurements of the two first columns of the table. Since the maximum delay in transmission and reception is 3198 μs and 3162 μs respectively, a value of 4000 μs is selected for τ. This time is sufficient to ensure a proper algorithm operation. As a result, a new common delay for transmitter and receiver can be observed in the third and fourth columns of the table. Note that this delay (4042 μs) is slightly higher than 4000 μs;

Table 1
Mean (*mean*) standard deviations (*sdev*) maximum (*max*) and minimum (*min*) values of the delay between the start of processing routine and the effective activation of the processing interrupt for transmitter (*Tx*) and receiver (*Rx*) configurations. (A) without compensation and (B) with delay compensation as described in Section 4.

	(A) $t_{int} - t_{ref}$		(B) $t'_{ref} - t_{ref}$	
	Tx	*Rx*	*Tx*	*Rx*
Mean (μs)	2148.88	2192.20	4042.01	4042.00
Sdev (μs)	487.63	494.65	0.42	0.41
Min (μs)	1252	1241	4041	4041
Max (μs)	3198	3162	4043	4043

which is due to a fixed number of operation cycles needed by the microcontroller to set up the τ delay.

Consider first the situation in which no compensation is used (experiment A), whose corresponding values are shown in the two first columns of the table. Mean delay values are around 2.1 ms and 2.2 ms for transmitter and receiver nodes respectively. However an important random behavior is also observed with a standard deviation of around 0.5 ms. By considering a typical 340 m/s value for the speed of sound, this leads to rms distance errors of around 17 cm.

When using the proposed compensation scheme (experiment B) this random behavior is greatly reduced. Mean values, standard deviations and minimum and maximum values for this situation are shown in last two columns of the table. In this case, mean values are the same for nodes configured as transmitters or receivers. Moreover, maximum absolute deviation around the mean value is of only 1 μs (the nominal clock resolution) and the standard deviation reduces to 0.41 μs (the theoretical minimum value for the used clock resolution). Therefore, rms distance errors due to the clock synchronization are now reduced to 0.14 mm, which is more than adequate for a sub-centimeter system.

6.2. Clock drift compensation

An evaluation of the relative clock drifts was performed by averaging the estimation (11) over a set of 500 synchronization messages for each node. Results in ppm are shown in the first column of Table 2. Drift values with respect to other nodes are computed using (10) and shown in columns N1–N5 of the table. Most node combination exhibit relative small drift values below 10 ppm relative to the coordinator clock with the exception of node N3 which exhibits a −64.91 ppm drift. This is probably because this node (or the included quartz crystal) belongs to a different production series.

Fig. 6 qualitatively shows the effect of clock drift in TOF measurements. Values are obtained using a pair of nodes, N1 configured as transmitter and N2 as receiver. Measurements have been obtained using the setup shown in Fig. 5. The distance between the nodes was approximately 3.5 m. The sampling frequency for the digital detector was selected as 17.78 kHz. The system was scheduled to perform 32 measurements in each multiframe (one measurement every frame). Filled dots correspond to TOF measurements obtained without drift compensation, and unfilled dots correspond to measures obtained after applying the proposed clock drift compensation algorithm.

Table 2
Estimated drift values of each node clock with respect to each other. Values are in ppm. First column (NC) show the estimated drifts of all nodes with respect to the coordinator clock. Other columns show the estimated drift values with respect to the other nodes clock.

	NC	N1	N2	N3	N4	N5
N1	0.11	0.00	8.61	65.02	7.35	1.04
N2	−8.50	−8.61	0.00	56.41	−1.26	−7.57
N3	−64.91	−65.02	−56.41	0.00	−57.67	−63.98
N4	−7.24	−7.35	1.26	57.67	0.00	−6.31
N5	−0.93	−1.04	7.57	63.98	6.31	0.00

In the first case, the TOF error increases linearly with time and is reset at the beginning of every new multiframe. This is because a resynchronization occurs at the reception of a new synchronization message sent by the coordinator at the beginning of every multiframe. From Table 2, the N1 node drift relative to the N2 node clock is 8.61 ppm. The maximum TOF error occurs at the beginning of the last frame which is 6.2 s from the beginning of the multiframe. Therefore, the expected value of this error will be $6.2\ s \times 8.61 \times 10^{-6} = 53.4\ \mu s$ which explains the difference between maximum and minimum TOF values in Fig. 6. The standard deviation of TOF values is in this case 16.02 μs yielding to a pseudorange rms error of 5.44 mm at 340 m/s. When the clock drift compensation is applied (unfilled dots) the error due to the clock drifts is removed and now the standard deviation of TOF is only 1.34 μs which corresponds to a rms pseudorange error of only 0.45 mm.

To quantitatively validate the proposed synchronization scheme, a set of TOF measurement was performed for four different pair of nodes. In this case, N1 node was configured as transmitter and nodes N2, N3, N4 and N5 where configured as receivers. As in the previous case the system was scheduled to perform 32 measurements per multiframe. The separation between nodes was approximately 3.5 m. For each pair of nodes, 1600 TOF measurements where recorded in two different scenarios: without clock drift compensation (A) and with the proposed compensation scheme (B). Mean and standard deviation values for the measured TOF are shown in Table 3.

For the experiment A when no drift compensation is used, the standard deviation of TOF measurements is dominated by the synchronization error caused by the clock drifts. Nodes N2, N4 and N5 exhibit relative small drifts and therefore the standard deviation of the TOF is small (less than 16.1 μs or a pseudorange rms error of 5.47 mm). Nevertheless node N3, due to its greater drift, exhibits a standard deviation as large as 120.72 μs which correspond to a pseudorange rms error of 4.1 cm. However, when the proposed compensation technique is applied (experiment B), standard deviations of all nodes are reduced to values less than 1.4 μs, which corresponds to a pseudorange rms error of about 0.48 mm.

Note that these errors are higher than the theoretical limit calculated for a perfect synchronized system with a time resolution of 1 μs (on the order of 0.14 mm). The residual errors are caused by other effects such as low SNR values and multipath caused by reflection of the ultrasonic signal in floor and walls. In any case, the results of this last experiment show that the proposed algorithm is able to improve the accuracy of the TOF measurement by removing synchronization errors allowing sub-centimeter accuracies.

6.3. Relevant TELIAMADE features

In this section, we show a summary of the most relevant features of the proposed TOF measurement technique

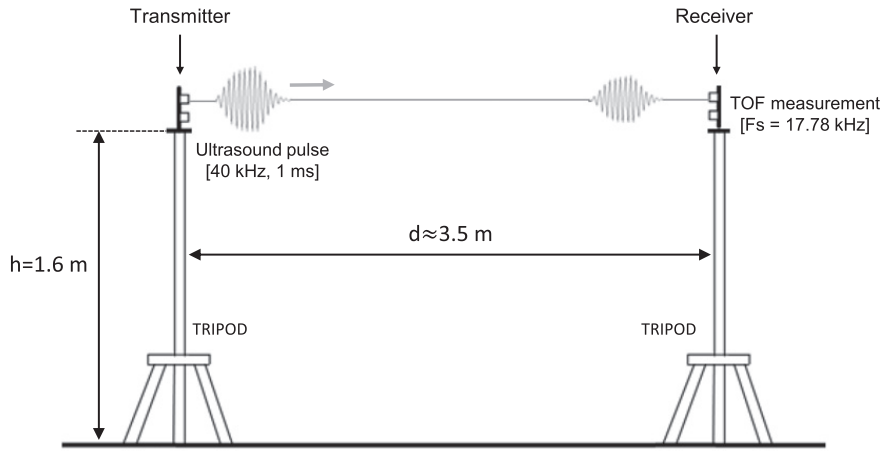

Fig. 5. Illustration of the test-bed used in the pseudorange measurements. A transmitter node and a receiver node are placed one in front of the other using a pair of tripods to a height of 1.6 m above the ground. The distance between nodes is set to 3.5 m approximately. The transmitter node sends periodically an ultrasound pulse of 1 ms at the beginning of each frame of the multiframe. In this way 32 measurements of pseudorange are recorded in the receiver node in each multiframe period (T_M), using a sampling frequency of 17.78 kHz.

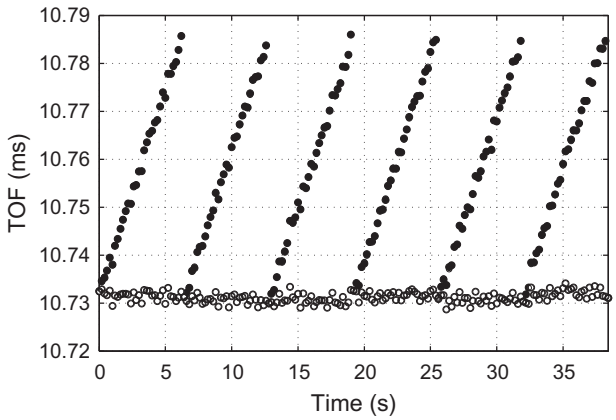

Fig. 6. TOF estimations using a couple of network nodes (N1 transmitter and N2 receiver) at an approximate distance of 3.5 m using a sampling frequency (reception) of 17.78 kHz. Filled dots correspond to measures without clock drift compensation. Unfilled dots correspond to measures after applying the clock drift compensation.

Table 3
Mean value (*mean*) standard deviation (*sdev*) of TOF measurements between four pair of nodes. Node N1 is configured as transmitter and N2, N3, N4 and N5 as receivers. Distance between transmitter and receiver nodes is about 3.5 m and sampling frequency is fixed at 17.78 kHz. Experiment A: Results without compensation and experiment B: Results with the proposed clock drift compensation.

	TOF	N1–N2	N1–N3	N1–N4	N1–N5
A	*Mean* (μs)	10738.32	10886.56	10706.98	10685.67
	Sdev (μs)	16.08	120.72	12.92	2.33
B	*Mean* (μs)	10731.67	10684.23	10685.40	10682.46
	Sdev (μs)	1.22	1.15	1.26	1.39

along with a comparison to other approaches found in the literature.

The approach followed for TELIAMADE nodes design is to incorporate ultrasonic TOF measurement capabilities to existing ZigBee devices. The base hardware is a low power radio modem (CC2420) and a low power microcontroller (PIC17F4620). The ZigBee protocol stack is implemented by the microcontroller. The additional hardware is minimized as shown in Section 2. It only includes a pair of low cost narrowband ultrasonic transducers (400ST/R120), one digital inverter chip (MC14049UB) and a dual operational amplifier (LMC648IN) along with some passive components. The cost of this additional hardware is very low in comparison with the ZigBee base hardware. In addition, TELIAMADE nodes are battery powered, with a voltage between 2.7 and 3.6 V. Generation and detection of ultrasonic signals is performed digitally, and therefore any TELIAMADE node can be configured by software to operate either as an emitter or receiver of ultrasonic signals. In the last case, the node can itself perform the TOF estimation without the intervention of any other network node.

In most positioning systems found in the literature (Cricket ActiveBat, Dolphin, 3D-locus) the mobile nodes are wireless. By contrast, the reference nodes (beacons) have wired connections. In TELIAMADE however, all nodes are wireless. The design of TELIAMADE is very attractive from the standpoint of system implementation, as it prevents the cable connections of the beacons. This wireless design however raises a problem of time synchronization of the TOF measurements. The problem was solved in the above systems by using a specific radio interface for synchronization. For example, the mobile node in 3D-LOCUS is equipped with a radio interface in the 433 MHz band for synchronization and a Bluetooth radio interface to transfer data to the central node that performs the estimation of the TOF. In this approach, each measurement is signaled through the transmission of an RF pulse. By contrast, TELIAMADE nodes use the same interface for data transmission and for synchronization purposes, which simplifies the design and reduces the cost and the power consumption of the nodes. When using the proposed TDMA measurement scheduling, the average power consumption of a TELIAMADE node is of 10 mA for a typical scenario with a rate of 5 TOF measurements per second; and of only 1.7 mA in idle mode. When powered by a typical 2000 mA h battery, the half-life of the battery will be around 200 and 1176 h respectively.

3D-LOCUS uses a BPSK modulated signal with a Gloay spreading code. The bandwidth used is from 5 kHz to 25 kHz. A digital correlation detector is used that operates at a sampling frequency of 150 kHz. Due to the high processing resources; the correlation detector is implemented in a central node, equipped with a DSP (Texas Instruments 150 MHz F2812 DSP). The reported pseudorange precision is of 0.22 mm for a distance of 68 mm between nodes (emitter and receiver). In our system, ultrasonic pulses of 1 ms are used instead, with an occupied bandwidth of only 2 kHz. Although the carrier frequency of the ultrasonic signal is of 40 kHz, the use of a band-pass sampling scheme allows to sample the ultrasonic signal at frequencies as low as 17.7 kHz. This greatly reduces the needed computational resources and allows the receptor node to implement the correlation detector, avoiding the need of a central node to perform the TOF estimation. Anyway, a pseudorange precision of 0.44 mm is achieved at a 6 m separation between transmitter and receiver. This is comparable to the one reported for 3D-LOCUS with a much simpler system.

7. Conclusions

In this paper, the problem of obtaining time-synchronous measures in a wireless sensor network is addressed. In particular, IEEE 802.15.4 based networks using the ZigBee protocol are considered. Unlike other synchronization schemes proposed in the literature, our system uses the same radio interface for both data transmission and synchronization purposes. Network synchronization is achieved through the time-stamps of transmission and reception of network packets, for which modifying the MAC layer of the protocol was necessary. The proposed algorithm is based on a TDMA structure which significantly reduces the traffic of synchronization packets over the network and consequently the power consumption. In addition, this approach allows performing periodically scheduled measures without the intervention of the network coordinator. This approach has several problems related to maintaining an adequate synchronization that are also investigated in the paper. In particular de-synchronization due to different processing times in network nodes and clock drifts are characterized, and algorithms to compensate for these effects are presented.

The proposed synchronization algorithm is implemented and evaluated in a local positioning system based on ultrasonic time-of-flight estimations. The system is composed by a set of fixed nodes that act as ultrasonic transmitters and one or more mobile nodes acting as ultrasonic receivers. Experimental results demonstrate the high precision of the proposed system, which makes it a very attractive approach for these kinds of positioning systems and other applications in which a precise time synchronization is required.

Acknowledgements

This work was partly supported by the Junta de Andalucía under Research Project P08-TIC-03886. Authors are with the Dept. of Signal Theory, Telematics and Communications of the University of Granada (TSTC–UGR) and with the Information and Communications Technology Research Centre (CITIC–UGR).

References

[1] C. Medina, J.C. Segura, A. de la Torre, TELIAMADE: Sistema de localización en interiores basado en ultrasonido y RF, in: XXV Simposium nacional de la URSI, 2010, p. 39.
[2] C. Medina, J.C. Segura, A. de la Torre, Una red inalámbrica de sensores orientada a localización con precisión subcentimétrica, in: XXVI Simposium nacional de la URSI, 2011.
[3] ZigBee Alliance, Zigbee protocol specification, 2007. <http://www.zigbee.org>.
[4] IEEE std. 802.15.4-2003, Wireless Medium Access Control (MAC) and Physical Layer (PHY) specifications for Low Rate Wireless Personal Area Networks (LR-WPANs). <http://www.ieee802.org/15/pub/TG4.html>.
[5] C. Falsi, D. Dardari, L. Mucchi, M.Z.Win, Time of arrival estimation for UWB localizers in realistic environments, EURASIP Journal on Applied Signal Processing 2006 (2006) 13 (ID 32082).
[6] P. Bahl, V. Padmanabhan, RADAR: an in-building RF-based user location and tracking system, in: Proc. IEEE Infocom 2000, IEEE CS press, Los Alamitos, California, 2000, pp. 775–784.
[7] T.A. Alhmiedat, S.-H. Yang, A ZigBee-based mobile tracking system through wireless sensor networks, International Journal of Advanced Mechatronic Systems 1 (1) (2008) 63–70.
[8] L.M. Ni, Y. Liu, Y.C. Lau, A.P. Patil, Landmark: Indoor location sensing using active RFID, Wireless Networks. Special Issue on Pervasive Computing and Communications 10 (6) (2004) 701–710.
[9] J. Krumm, S. Harris, B. Meyers, B. Brumitt, M. Hale, S. Shafer, Multi-camera multiperson tracking for easyliving, in: Proc. 3rd IEE E Int. Workshop on Visual Surveillance, IEEE CS press, Dublin, Ireland, 2000, pp. 3–10.
[10] E. González, L. Prados, A. Rubio, J.C. Segura, A. de la Torre, J. Moya, P. Rodríguez, J. Martfn, ATLINTIDA: a robust indoor ultrasound location system: design and evaluation, in: J. Corchado, D. Tapia, J. Bravo (Eds.), 3rd Symposium of Ubiquitous Computing and Ambient Intelligence 2008, Advances in Soft Computing, vol. 51, Springer, Berlin/ Heidelberg, 2009, pp. 180–190.
[11] A. Harter, A. Hopper, P. Steggles, A. Ward, P. Webster, The anatomy of a contex-aware application, in: Proc. of the 5th Annual ACM/IEEE Int. Conf. on Mobile Computing and Networking (Mobicom 1999), 1999, pp. 1–59.
[12] N.B. Priyantha, A. Chakraborty, H. Balakrishnan, The CRICKET location-support system, in: Proc. 6th ACM MOBICOM, ACM press, New York, 2000, pp. 32–43.
[13] M. Hazas, A. Hopper, Broadband ultrasonic location systems for improved indoor positioning, IEEE transactions on mobile computing 5 (5) (2006) 536–547.
[14] J.C. Prieto, A.R. JimTnez, J.I. Guevara, J.L. Ealo, F.A. Seco, J.O. Roa, F. Ramos, Subcentimeter-accuracy location through broad-band acoustic transducers, in: Proc. IEEE Int. Symp. Intell. Signal Processing, 2007, pp. 929–934.
[15] J.C. Prieto, A.R. Jimenez, J.L. Ealo, F. Seco, J.O. Roa, F. Ramos, Performance evaluation of 3D-LOCUS advanced acoustic LPS, *IEEE transactions on instrumentation and measurement* 58 (8) (2009) 2385–2395.
[16] Microchip, 28/40/44-Pin Enhanced Flash Microcontrollers with 10-Bit *A/D* and nanoWatt Technology. <http://ww1.microchip.com/downloads/en/DeviceDoc/39626e.pdf>.
[17] Texas Instruments, CC2420 2.4 GHz IEEE 802.15.4/ ZigBee-ready RF Transceiver. <http://www.ti.com/lit/ds/symlink/cc2420.pdf>.
[18] Prowave, 400S12.PDF400ST120/SR120 data sheet. <http://www.prowave.com.tw/pdf/T400S12.PDF>.
[19] O. Semiconductor, MC14049UB data sheet. <http://www.datasheetcatalog.org/datasheet/on_semiconductor/MC14049UB-D.PDF>.
[20] N. Semiconductor, LMC6482IN. <http://www.ti.com/lit/ds/snos674c/snos674c.pdf>.
[21] W.M. Waters, B.R. Harret, Bandpass signal sampling and coherent detection, IEEE Transactions on Aerospace and Electronic Systems AES 18 (4) (1982) 731–736.
[22] J.L. Brown Jr., On quadrature sampling of bandpass signals, IEEE Transactions on Aerospace and Electronic Systems AES 15 (3) (1979) 366–371.
[23] J.L. Brown Jr., Digital time-of-flight measurement for ultrasoinc sensors, IEEE Transactions on Instrumentation and Measurement 42 (1) (1992) 93–97.

[24] M. Mock, R. Frings, E. Nett, S. Trikaliotis, Continuous clock synchronization in wireless real-time applications, in: Proc. of the 19th IEEE Symposium on Reliable Distributed System (SRDS-00), 2000, pp. 125–133.

Carlos Medina is a Ph.D. student at the Department of Signal Theory, Telematics and Communications of the University of Granada (Spain). He obtained his B.S. degree in Telecommunications Engineering from the University of Granada in 2008, and his M.S. in Multimedia Systems also from the University of Granada in 2009. He was granted a Ph.D. fellowship by the Andalusian Regional Government on September 2009 and started his Ph.D. studies. His research interests include wireless sensor networks and indoors positioning systems based on ultrasound and radio-frequency.

Jose C. Segura obtained an M.S. in physics from the University of Granada, Spain, in 1984 and a PhD. in variants of HMM modeling for speech from the University of Granada in 1991. He is full professor of Signal Theory and Communications at the department of Signal Theory, Telematics and Communications of the University of Granada, and vice director of the Research Centre on Information Technologies and Communications (CITIC-UGR) of the University of Granada. He was previously assistant professor of Electronics at the Department of Electronics and Computer Technology, University of Granada, and vice director of the Centre for Information Services and Communications of the University of Granada. His current research interests include ultrasonic signal processing, sensor networks, signal processing, communication systems, and speech recognition. He is senior member of IEEE and reviewer for several scientific journals.

Á**ngel de la Torre** received the M.Sc and Ph.D. degrees in physics from the University of Granada, Granada, Spain, in 1994 and 1999, respectively. Since 1994, he has been working with the Research Group on Signals, Telematics and Communications, Department of Signal Processing, Telematics and Communications, University of Granada. In 2000, he joined the PAROLE Group, Laboratoire RFIA du LORIA, Nancy, France, as a Postdoctoral Researcher in the field of robust speech recognition, and the Institut für Angewandte Physik, Innsbruck, Austria, as a Postdoctoral Researcher in the field of cochlear implants. Since 2003, he has been an Associate Professor with the University of Granada. His research interests are in the field of signal processing, and particularly robust speech recognition, speech processing in noise conditions, signal processing for cochlear implants, processing of seismic signals, acquisition and processing of electrophysiological responses in audiology and processing of mass spectrometry data. He is reviewer for several scientific journals.